Hardening Doppler Global Velocimetry Systems for Large Wind Tunnel Applications

James F. Meyers*
Joseph W. Lee**
Mark T. Fletcher**
Bruce W. South**

Fluid Mechanics and Acoustics Division
NASA Langley Research Center
Hampton, Virginia 23681-0001 USA

ABSTRACT

The development of Doppler Global Velocimetry from a laboratory curiosity to a wind tunnel instrumentation system is discussed. This development includes system advancements from a single velocity component to simultaneous three components, and from a steady state to instantaneous measurement. Improvements to system control and stability are discussed along with solutions to real world problems encountered in the wind tunnel. This on-going development program follows the cyclic evolution of understanding the physics of the technology, development of solutions, laboratory and wind tunnel testing, and reevaluation of the physics based on the test results.

INTRODUCTION

The development of classical wind tunnel instrumentation proceeded from the origination of the basic concept, to the development of a mathematical model to determine feasibility, followed by the construction of a laboratory prototype. The prototype would subsequently be tested to determine if the instrument yielded the desired measurement. Then a first generation system would be constructed and tested in a wind tunnel. Its performance would be evaluated by comparing the results with theoretical predictions and/or measurements obtained with other instrumentation. Typically, the new technology would have the same performance in the wind tunnel as it did in the laboratory.

While the development of Doppler Global Velocimetry (DGV) followed this sequence, the expected wind tunnel performance, as predicted by laboratory testing, has not yet been realized. The instrument has proven to be very sensitive to environmental conditions. Additionally,

efficient operation of DGV requires modifications to normal wind tunnel testing procedures. This instrument promised measurement capabilities unparalleled by current flow field measurement technologies to provide the large experimental databases needed to verify computational fluid dynamic codes. In addition, this global measurement technology had the potential to reduce the test time needed to globally describe complex flows.

The laboratory development phase of DGV was thus expanded to include wind tunnel testing to guide and supplement laboratory investigations. This expanded development program provided greater insight into the fundamental characteristics and sensitivities of the technology. DGV has been tested in subsonic, transonic, and supersonic flows in wind tunnels spanning the laboratory-type Basic Aerodynamics Research Tunnel at Langley to the large 40-by 80-foot National Subsonic Tunnel at the NASA Ames Research Center. Each of these wind tunnel entries revealed aspects of the technology that were later refined in the laboratory. Once understood, the system and/or data processing software were modified to minimize environmental sensitivity while maximizing measurement resolution and accuracy. This process, which continues today, is described here.

Early System Development

Doppler Global Velocimetry was invented when Komine[1] used the light absorption characteristics of Iodine vapor to determine the absolute frequency of Doppler shifted laser light scattered by small particles passing through an Argon ion laser beam. With the laser frequency tuned to the midpoint along the side of the absorption line, Doppler shifted scattered light would pass through the Iodine vapor with greater (or less, depending on the direction of the Doppler shift) absorption, thus establishing the fundamental measurement relationship. Since Doppler-shifted scattered light is the measurement parameter, DGV does not require optical resolution of individual seeding particles, nor is it limited to the measurement of velocity at a single location in space. The direct measure of optical frequency eliminates the problems of signal interference from multiple scatterers inherent in standard laser velocimetry. Thus collected scattered light originating from a particle cloud passing through the spatial volume subtended by the laser beam and the viewing receiver optical system will yield the average velocity of the scattering particles present within the volume. A global measurement system can then be constructed by expanding the laser beam into a light sheet and replacing the detectors with Charge Coupled Device (CCD) video cameras, Figure 1. Each pixel element of the CCD becomes, in effect, a single detector measuring the average velocity within the portion of the light sheet imaged on that pixel. Thus

the signal camera image, following normalization by a reference camera image, becomes a picture of the velocity field.

The trivial mathematical description and subsequent measure of a supersonic jet in the laboratory by Komine *et al* [2] and the velocity field measurement of a rotating wheel by Meyers and Komine[3] lead directly to the construction of the first generation wind tunnel DGV system. The optical configuration is shown in schematic form in Figure 1 and pictorially in Figure 2. A custom video electronics system was constructed to normalize the signal camera to the reference camera. The resulting RS-170 compatible signal was processed by a commercial frame grabber to produce real-time pseudo colored video to better visualize the velocity field. The first DGV wind tunnel application was the measure of the vortical flow above a delta wing in the Langley Basic Aerodynamic Research Tunnel, Figure 3. While the normalized signal images gave an indication of velocity dependency, the data quality from laboratory measurements of a rotating wheel was not obtained. Subsequent laboratory investigations traced the poor data quality to the inability to perfectly align the two cameras. Normalized images obtained from perfectly aligned cameras would produce a constant amplitude throughout the image, even if the target was a series of black dots on a white background. An alignment error would produce a series of shadows on the same side of all the dots. Optical distortions caused by the components in the receiver optical system would produce shadow patterns that vary within the image[4], Figure 4. This inability to overlay the two images within subpixel tolerances results in the incorrect calculation of normalized amplitudes, since the corresponding signal and reference pixels view different locations in the light sheet. Image processing techniques were used to realign the distorted images. These tools also removed the perspective distortions imposed on the images when viewing the light sheet from the side of the wind tunnel, Figure 2.

Implementation of this technology required the digital acquisition of each camera output, and the development of new calibration procedures and data processing software. A survey of commercial frame grabbers did not find a system that was capable of acquiring images simultaneously from multiple cameras. Thus a custom dual frame grabber was constructed[3]. An alignment target, consisting of a two-dimensional array of equispaced dots, was also constructed. The dots on this target also served as the fiducial marks required by commercially-available image processing software to determine the warping equations needed to de-warp the images. Normalization of the warped signal and reference target images still showed shadows about the dots indicating incomplete removal of the distortions. The commercial software was able to remove linear distortions such as perspective, but was incapable of removing the effects of minor, nonlinear distortions originating from optical imperfections. A software-development program was undertaken to obtain warping algorithms that were capable of removing both perspective and optical distortions. The resulting method used piecewise, bilinear warping procedures

to subdivide the target image into sections sufficiently small to approximate the nonlinear distortions by linear segments[5]. In practice, a grid of 20 by 20 sections, defined by the dot centroids in the test target, yielded sufficient correction[4].

Other system modifications derived from the delta wing test include revised light sheet forming optics and optics to reduce Mie scattering effects. The light-sheet-forming cylindrical lens was replaced with a high-speed galvanometer scanner to produce a light sheet with a more uniform intensity distribution. Scattering-angle and polarization-dependent Mie scattering intensity variations[6] were reduced by placing a quarter-wave plate in the laser output beam to circularize the laser light polarization.

The vortical flow field above the delta wing was again measured using the revised optical system, new digital acquisition system, and improved data processing software. The resulting measurement of the cross-flow velocity component is shown in Figure 5. The structure on the left side of Figure 5 is characteristic of a vortical flow, whereas the structure on the right is representative of a solid body of revolution. The laser light sheet was rotated to align with the vortex path, Figure 6. The illuminated smoke on the left side of the delta clearly shows a dark region indicative of a vortical core extending along the full length of the delta. The dark core region on the right side ends in a homogeneous cloud near the front of the delta indicating that the vortex has burst. Since the DGV measurements were acquired at 80-percent chord, Figure 5 shows the velocity field of the burst and unburst vortices.

Modifications to the DGV System

Although the new test results showed a vast improvement in data quality, they also uncovered further noise sources and the next level of hardware problems. The data was noisy and contained unrealistic values at the edges of the smoke plume. Further analysis of the data and the operation of the CCD video cameras revealed several system characteristics that could be responsible. These include:

1) camera dark current,
2) stray ambient room light,
3) stray laser light scattered from structures including the model,
4) variations in pixel sensitivity throughout the CCD array,
5) charge transfer noise, modulation transfer function, and
6) field interlacing.

Spatially dependent variations in light transmission through the signal and reference optical paths were also discovered. These

variations were caused by nonuniform optical transmission/reflection from the beamsplitter, mirror, and the Iodine vapor cell windows, resulting from manufacturing defects, and even dirt on the optics. Severe optical distortions were present in the signal and reference camera images. The distortions were traced to the use of the image transfer optical configuration in the receiver optical system, and stresses induced by welding thin windows to the Iodine vapor cell body.

These findings led to the development of new calibration procedures, changes and additions to the data processing software, and modifications and replacements in the receiver optical system[4]. First, the assumed linearity of the CCD video cameras was verified. The linear response allowed the pixel sensitivity map to be resolved by illuminating the CCD with two intensities of green light. The sensitivity slope (quantum efficiency) for each pixel was then computed. Background light images were acquired with the DGV system operating normally, except smoke was not injected into the flow. Subtracting these images from the data images would remove contributions from background room and laser light along with camera dark current. The data acquisition software was modified to accept only a single field from the acquired data frames because the second field was obtained after the first field was acquired. Linear interpolation methods were used to estimate the missing interlaced rows. Charge transfer noise was reduced using standard kernel-based low pass filtering techniques. A 5x5 top hat filtering kernel was chosen because its bandwidth was slightly wider than the modulation transfer function of the cameras. Thus, high-frequency noise was removed without influencing the characteristics of the measured flow structures.

A new calibration procedure was added to determine the spatially dependent variations in light transmission through the signal and reference optical paths. A flat white target was placed in the laser light sheet plane and data images acquired. The ratio of the reference image divided by the signal image become a correcting map to spatially flatten the optical transmission of the receiver optical system.

The receiver optical system was restructured from the image transfer configuration to the boresight configuration. This change increased optical transfer efficiency and eliminated the severe optical distortions imposed by the short focal length transfer lens. A second receiver optical system was constructed for the purpose of measuring the laser output frequency. This laser frequency monitor was necessary because the optical frequency would slowly drift with time. The laser would also occasionally hop longitudinal modes that suddenly changed the optical frequency by 126 MHz in the 5 W Argon ion laser. Finally, the NASA-built Iodine vapor cell was replaced by a commercial unit that had thick optically flat windows. These windows were cold welded to the cell body, thus eliminating the image distortion problems

found in the NASA cell. The new cell was also manufactured using a multi-purge method with inert nitrogen to insure complete removal of contaminating oxygen. A second commercial cell was obtained and installed in the laser frequency monitor.

The loop completed with the next wind tunnel test ¾ an investigation of the supersonic flow in the Langley Unitary Plan Wind Tunnel[7]. The measurement of the vertical velocity component above an inclined flat plate at a freestream Mach number of 2.5 is shown in Figure 7. The variation in velocity above the shock is the contribution of freestream. As the scanning galvanometer swept the laser beam upstream and downstream of the orthogonal viewing direction, freestream velocity contributed to the measurement vector by the sine of the sweep angle. This investigation also provided the opportunity to determine the capability of DGV to obtain measurements from submicron diameter water condensation particles.

The Three Dimensional System

The conflict between desired light sheet orientations and the basic Doppler relationship prohibits the measurement of velocity in standard Cartesian coordinates. Thus, three component DGV measurements were necessary to resolve flow velocity along the standard coordinate axes. Previously, sequential three-component measurements were obtained by reorienting the light sheet within the measurement plane[5]. These measurements could be resolved along standard axes, but flow stationarity and measurement independence must be assumed. A better solution would be the addition of two receiver optical systems to obtain simultaneous three component measurements. The data acquisition system was also upgraded from the NASA-built dual frame grabber to a commercial image processing system capable of acquiring simultaneous data from six RS-170 video cameras.

The next development loop began again in the laboratory where two questions needed to be answered: Is the warping technology sufficiently accurate to overlay six camera images with the necessary precision to obtain velocity vector transformations? Can resolved measurements be obtained should the receiver optical systems move with respect to one another?

The three-component DGV optical system was placed about a rotating wheel, with a receiver set on the left, the right, and above with a 30^{o} inclination to the plane of the wheel. The wheel was illuminated with a cone of laser light propagating in the horizontal plane, and inclined by 45^{o} to the wheel. The view from each receiver of the calibration dot card placed on the wheel is shown in Figure 8. Warping these three images to remove perspective and optical distortions produced the squared images also shown in Figure 8. Spatial

alignment of the three images was set by locating the fiducial dot, representing the center of the wheel, to the same pixel location in the output images. Magnification of each image was adjusted to yield the same number of rows and columns extending from the fiducial dot. The three warped images appear to have the proper overlay to determine the normal streamwise, U (orthogonal to the wheel), cross flow, V (horizontal), and vertical, W velocity components for each corresponding pixel in the images.

The wheel was spun and the velocity data acquired. The measured and resolved velocity images are shown in Figure 9. As expected, the U component was nominally 0 m/s, and the V and W components had the appropriate profiles for a solid body of revolution, with the proper 90^{o} phase difference between them. The wheel was then moved 1.0 cm away from the receiver optical systems along the streamwise direction. This change had the effect of misaligning the three receiver optical systems with respect to one another. Again the wheel was spun and velocity data acquired. The acquired images were processed in the same manner using the same warping equations as before. This was acceptable since the optical distortions did not move, and the wheel was still within each camera depth of field. Thus components A, B, and C yielded the same velocity measurements as before except the data was spatially shifted. These three images were realigned by cross correlating their respective reference camera images to determine the spatial offsets. After aligning the component images, the orthogonal components were resolved. The results were the same as before except the edges of the wheel were clipped because of a smaller common area.

The next step was the attempt to transfer this technique to the wind tunnel. The first wind tunnel application of the three-component DGV system served as a demonstration of the Langley-designed system for the 40-x 80-foot National Subsonic Wind Tunnel at the NASA Ames Research Center[8]. The high-temperature (700^{o} C), high-speed (500 m/s) flow exiting an engine model at component focal distances up to 15.5 m constituted a test of the de-warping techniques. Cross-correlating the component measurements was not necessary because of the stability of the system installation. Unfortunately this was not true for the next wind tunnel test ¾ the investigation of the wing tip vortex interaction with a trailing model in the Langley 30-x 60-foot Full Scale Wind Tunnel, Figure 10. Although this facility was smaller than the Ames tunnel, it had an open test section making the optical system installation more difficult. Two of the receiving optical systems were installed in pods on the test section floor, (Figure 10), at focal distances of 7.5 m from the light sheet. The third receiver was placed on top of the test section inlet at a focal distance of 18.25 m. A 5-cm diameter vortical flow was measured with the upstream airfoil set to 2- and 10-degree angles of attack. As expected, system vibration from flow buffeting and tunnel vibration affected system alignment. Cross correlating each component signal image with its respective reference image showed component misalignments up to 3 pixels (3.75 mm in the measurement plane). Component-to-component misalignments were found to be as great as 10 pixels

(12.5 mm in the measurement plane). The component measurement images were computed following the alignment of each signal camera image with respect to its reference camera image. These images were then aligned to resolve the orthogonal velocity components. Averaging 30 cross-flow velocity data images produced the results shown in Figure 11 for the two angles of attack. Although these results clearly show the vortex motion, they provide little information about the vortex structure. Applying the cross correlation procedure to the 30 data images compensated for vortex motion and produced the averaged vortex structures shown in Figure 12. These two wind tunnel tests showed that three-component DGV measurements were possible in large wind tunnels.

Instantaneous Measurements

To date, the DGV systems used a continuous-wave Argon-ion laser and free-running, industry-standard RS-170 CCD video cameras. Allowing the cameras to free run at their 16.7 ms single-field integration time maximized the acquired scattered light. While this long integration time was satisfactory for the measurement of stationary flows, it was unacceptable for the measurement of unsteady flow fields such, as in rotorcraft applications. In anticipation of the need for a pulsed system, the Northrop Research and Technology Center was contracted by the NASA Langley Research Center in 1990[9], to conduct laboratory investigations to determine if a pulsed, single-frequency, frequency-doubled Nd:YAG laser could be used in DGV applications to obtain instantaneous velocity measurements. This successful research program culminated with the first instantaneous DGV measurements, the one-component velocity measurements in a 10-x 10-cm jet.

The first wind tunnel use of the instantaneous DGV system was chosen to be the azimuth dependent measurement of a helicopter rotor wake. The flow would have been generated by an isolated rotor system consisting of a Mach-scaled, four bladed rotor with a rotor disk diameter of 1.7 m. The investigation was to be conducted in the Langley 14-by 22-Foot Subsonic Tunnel operating in the open test section configuration. Projection Moiré Interferometry (PMI) was selected to measure the rotor blade position, bending, and twist at the same instant as DGV measured the flow field. Additional test issues included: 1) the test would be conducted in winter; 2) the tunnel lights would be illuminated for rotor blade monitoring; and, 3) access to the test section would be prohibited during rotor operation.

These test requirements necessitated major redesigns of the DGV systems. This included:

1)Replacement of the continuous-wave Argon ion laser with a pulsed, single-frequency, frequency-doubled Nd:YAG laser;

2)Replacement of the scanning galvanometer with a cylindrical-lens light sheet forming optical system;

3)Replacement of the photodiodes in the laser frequency monitor with the same CCD video cameras used in the receiver optical systems;

4)Replacement of the data acquisition system with newer PC compatible frame grabbers capable of simultaneous acquisition from multiple cameras;

5)Development of new data acquisition and control software for the simultaneous acquisition of images from eight CCD video cameras at a 10 Hz rate. Four PC compatible computers acquired the data under the control of a master computer;

6)Encasing the Iodine vapor cells in insulated containers to minimize the effect of the expected large temperature changes in the wind tunnel;

7)Development of a temperature monitoring electronics system to acquire the stem and body temperatures of the Iodine vapor cells;

8)Development of timing and synchronization circuitry to control:

a)Nd:YAG laser,
b)PMI laser diode,
c)0.1 ms aperture electronic camera shutters (8 - DGV, 1 - PMI),
d)frame grabbers (8 - DGV, 1- PMI),
e)acquisition of Iodine vapor cell temperatures (8),
f)acquisition of rotor azimuth from the rotor shaft encoder;

9)Development of remote control beam directing optics to shift the Nd:YAG laser beam from the laser light sheet forming optics to Iodine vapor cell calibration optics.

The major part of the laboratory phase of this development was learning the characteristics of the Nd:YAG laser, constructing the new optical components, developing and constructing the new electronics systems, and developing the new software. The components were tested in the laboratory using actual equipment where possible, and simulated signals otherwise. The system was installed and tested in the 2-inch pipe flow facility as a rehearsal for the tunnel test.

Since the video acquisition systems were upgraded, a comparative study was undertaken to determine the tradeoffs between performance and cost of potential video systems. The performance criteria is camera signal-to-noise ratio. Camera manufacturers normally specify electronic signal to noise ratios during the acquisition of a single image. A more meaningful definition, from a measurement standpoint, is the image-to-image performance of the camera. That is, the ability of the camera to maintain a constant output level for each pixel from image-to-image with the camera viewing a constant illumination. A transparency composed of a series of gray-scale boxes of increased optical density was fabricated, Figure 13. Each camera / frame grabber under test acquired 100 images of the back lit transparency. A 10-x 10-pixel element was selected from each of the 10 boxes. The mean and standard deviation were calculated for each pixel within the element throughout the 100 images. The average of the 100 pixel mean values represented the signal, and the average of the 100 standard deviations represented the noise. The resulting signal-to-noise ratios for several camera / frame grabber sets are shown in Figure 14. Several conclusions were drawn from these results:

1) The frame grabber has a major influence on overall signal-to-noise ratio, e.g., the old RS-170 camera / 8-bit frame grabber yielded 6.5 effective bits in dynamic range whereas the same camera with a new PC compatible 10-bit frame grabber yielded 8.5 effective bits in dynamic range. (Frame grabber cost: $65k (old) versus $2k (new))

2) The 10-bit and 12-bit digital cameras yielded the same 8.5 effective bits in dynamic range.

3) The 16-bit digital camera yielded 9.5 effective bits in dynamic range.

4) High end cameras generally increased sensitivity with reduced noise at low signal levels, which is consistent with their primary design function in astronomical applications.

Based on these results, the RS-170 cameras were retained and the previous frame grabber was replaced with the 10-bit PC compatible frame grabber.

During system testing in the 2-inch pipe flow, the Iodine vapor cell temperatures would occasionally drift when environmental conditions changed. This problem was minimized after the cells were encased in insulated containers. However, it was not possible to simulate the environmental temperature changes expected in the wind tunnel. Elliot *et al*[10] and Roehle[11] reported that reducing the amount of Iodine contained in the cell to the point where all Iodine is in the vapor state resulted in more stable absorption line

calibrations. Once the Iodine was in the vapor state, increased temperature produced Doppler broadening, but no significant changes were found in the calibrations. A spare cell was overhauled by the manufacturer to yield full vapor at a cell temperature of 40^{o} C, the nominal cold point temperature setting of the standard cells. Laboratory testing of this cell produced calibrations far less temperature sensitive than other cells. Unfortunately, there was not sufficient time to overhaul the remaining cells before the tunnel test. The vapor limited cell was placed in the laser frequency monitor to increase stability of the laser frequency measurements.

INTEGRATION

The primary objective of the rotor wake experiment was to determine if three-component DGV technology could be used to measure the unsteady rotor wake flow field, and identify and characterize the vortical field within the wake. A second objective was to use the newly advanced capabilities of laser diode-based PMI system to obtain blade position, bending, and twist. The velocity and deformation data were acquired simultaneously, and in synchronization with rotor azimuth[12].

The isolated rotor test system is a ceiling-mounted general-purpose rotor testing system. The fully articulated hub holds a Mach-scaled, four-bladed, 1.7-meter diameter rotor. The rotor blades have a rectangular planform and an NACA 0012 airfoil section with a chord of 6.6 cm and a linear twist of -8 degrees, nose down. A digital, 1024 pulse per revolution encoder was attached to the rotor shaft to monitor rotor speed and provide an azimuthal record for conditionally sampling the instrumentation systems. A helicopter fuselage model was mounted on a vertical strut below the rotor. The strut could be raised and lowered to locate the fuselage in proper position under the rotor, Figure 15, or fully lowered to be out of the influence of the rotor wake. The housing containing the Nd:YAG laser and the laser frequency monitoring system, (along with one of the three receiver optical systems), can be seen outside the test section in Figure 15. The light sheet forming optics were located on the test section floor behind a flow deflector, Figure 15. Photographs of the light-sheet-forming optics and the receiver optical system are shown in Figures 16 and 17, respectively. All three receiver optical systems were placed on the advancing side of the rotor. They were positioned to have an unobstructed view of the laser light sheet when the fuselage was in place, Figure 18. The common field of view was an area 1.02-by 1.14-meters.

The PMI system was a single-component, laser diode based system capable of obtaining instantaneous (0.1 ms) measurements. This system is described in detail by Fleming and Gorton[13]. The system consists of a pulsed 15 W laser

diode bar (10 discrete emitters) operating at 800 nm, a Ronchi ruling, projecting optics, and an electronically shuttered CCD video camera. The laser diode bar was chosen as the light source because of its small size, high output power, single pulse operation, and infrared wavelength. The laser light passes through the Ronchi ruling (a diffracting grading with a square wave cross section) to a lens system that projected the resulting lines onto the underside of the rotor blades, Figure 19. The PMI optical system was placed below the test section floor to view a 1.2-by 1.2-meter area in the rotor disk plane covering 50 degrees of rotor azimuth, Figure 18. The data acquisition system, a one-camera version of the DGV component acquisition system, and the laser diode bar were triggered by the DGV synchronization signal. Thus the DGV and PMI systems acquired data at the same instant and each set to acquire data with the same measurement window.

Each day of testing began with the alignment of the DGV and PMI optical systems, followed by the spatial calibration of both systems at the desired span position. A rotor blade was removed during this process to allow unobstructed optical access to the dot target placed in the measurement plane. The laser light sheet was then aligned to the appropriate span position. Once aligned, the laser beam was redirected to the tunnel structure to conduct Iodine vapor cell calibrations. The rotor blade was replaced and the tunnel test section sealed. The rotor was spun to 2,000 rpm and the laser beam redirected to form the light sheet. Note that the rotor was always spinning when the pulsed light sheet was crossing the blades; this technique protected the composite rotor blades from damage by the high-power light sheet. The tunnel was then brought on line and free stream set to the desired velocity. A propylene glycol vaporization/condensation smoke generator was started and the smoke plume moved to pass through the measurement plane.

Data acquisition began when the rotor system, wind tunnel velocity, and smoke plume position were stable. A portion of the Nd:YAG laser beam was sampled by a fast photodiode with output monitored with a high-speed digital oscilloscope. The shape of the photodiode amplitude versus time trace was visually inspected to determine that the laser operated in single-frequency mode. If operating in single mode, a series of 100 conditionally sampled DGV and PMI image sets was acquired. The laser beam was then redirected to the tunnel walls and a sample of ten images was acquired to track the laser frequency in each receiver optical system. The light sheet was reformed and a second acquisition of 100 image sets obtained. Another laser frequency measurement was made followed by the acquisition of the third and final data set. The 300 conditionally sampled images sets would yield approximately 30 image sets at each of the selected azimuth angles: 0- to 90-degrees, every 10 ± 0.7 degrees.

ISSUES

The wind tunnel investigation had benefits and drawbacks. Full synchronization of the DGV and PMI systems was achieved with repeatable measurements as a function of rotor azimuth; both instruments operated simultaneously without interference; the DGV results match theoretical and experimental rotor wake skew angles; and, the PMI system successfully measured rotor blade position, bending, and twist. New problems included laser speckle noise; poor laser frequency stability; the inability of the Iodine vapor cell temperature management system to compensate for environmental changes; and partial coverage of the laser light sheet with seeding particles.

The rotor wake can be described as a cylindrical column of accelerated flow which is skewed from the freestream direction by an angle determined from the downward velocity within the wake and the freestream velocity magnitude. Figure 20 shows a DGV image of the freestream velocity component for a rotor position of zero degrees azimuth at the 27.7 m/s test condition. The view in the image is from the right side of the model looking inboard at the 80-percent radial location. The flow is from right to left and the rotor blade is rotating from left to right. The overlaid dot card pattern gives a sense of scale with 6.35 cm spacing between the dots. The skew angle obtained from the DGV data is shown in the figure along with the theoretical skew angle using the analysis of Stepniewski and Keys[18], and the flow visualization results obtained by Ghee *et al*[19].

The performance of the PMI system is illustrated by the progression of blade deformation measurements shown in figure 21. The rotor tip path plane was tilted 3 degrees nose down. The measured 26 mm difference in the blade tip deflection between 70 and 110 degrees of azimuth corresponds well to the expected deflection.

Changing the DGV laser source from the Argon-ion laser to a pulsed, single-frequency, frequency-doubled Nd:YAG laser provided the capability to obtain conditionally-sampled unsteady flow data. It also simplified Iodine vapor cell calibrations since the optical frequency was continuously tunable by controlling the injection laser voltage. Unfortunately, the change in laser also affected both image quality and frequency stability. Laser speckle was a far greater problem with the Nd:YAG laser than the Argon-ion laser. Although increased speckle might be expected from the narrower linewidth Argon-ion laser (10 MHz vs. 80 MHz for the Nd:YAG), the opposite was observed. The level of laser speckle noise expected from the Argon-ion laser was reduced by temporal averaging the collected particle-scattered light during the 16.7 ms CCD camera field integration time.

Classically laser speckle has been removed using low pass filtering techniques. These techniques include temporal averaging, spatial averaging, low frequency camera Modulation Transfer Functions (MTF)[14], data binning[15], and image convolution with a filtering kernel[16]. Temporal averaging of conditionally sampled instantaneous data requires an instrument stability greater than that achieved in the present study. The other techniques use hardware or software methods to spatially average the data images, thus smearing speckle noise. The speckle noise obtained when using the pulsed Nd:YAG laser was so severe, the filtering required to significantly lower the noise contribution would also mask the characteristics of flow structures. The data processing software developed for the Argon-ion based system used the image convolution technique, which when combined with normal temporal averaging, reduced the speckle noise to acceptable levels. However, the software was found to be completely inadequate for pulsed laser speckle. A new method was developed to remove laser speckle noise without modifying the measured flow structure.

A nonlinear filtering technique developed to remove impulse noise without affecting the underlying image integrity is the median filter[17]. Basically, the technique sorts pixel amplitudes within the processing kernel, e.g., 5x5 pixels, then selects the median amplitude as the filtered result. A median filter removes impulsive noise while the kernel-based low pass filter passes an impulse, albeit wider with a lower amplitude. The effectiveness of this filter can be seen by comparing a reference camera image with the image after filtering, Figure 22. Using this filtering method, laser speckle noise was virtually eliminated from the data images, revealing the rotor wake structures.

In the laboratory, the Nd:YAG laser maintained a stable output frequency with a small long term drift. In the wind tunnel however, severe temperature changes (20^{o} C) in the environment increased the rate of frequency drift. Induced vibrations from flow buffeting and tunnel structure motion caused the laser to change frequency randomly from pulse to pulse. For example, a series of ratio measurements obtained by the laser frequency monitor during the rotor wake investigation are shown in Figure 23 along with a similar series obtained during a subsequent investigation in the Langley Unitary Plan Wind Tunnel. A comparison of the two samples clearly shows the difference in laser performance between the laboratory-like conditions of the UPWT and the hostile environment of the 14-by 22-Foot Subsonic Tunnel.

The large changes in environmental temperature had the additional ramification of exceeding the capabilities of the Iodine vapor cell temperature management system. The effect can be seen by comparing the series of three Iodine cell calibrations taken during the course of a day's testing. For example, the calibrations for component C from a typical tunnel run are shown in Figure 24. The variation in the calibration resulted from temperature deviations in the cell from 47.4^{o} C, to 48.0^{o} C, to 53.0^{o} C respectively. This inability of the

temperature management system to maintain a constant temperature resulted in a variable bias error in the velocity measurements. In contrast, the vapor limited cell used in the laser frequency monitor yielded more stable calibrations, Figure 25, even though its temperature also varied.

Future Development

The rotorcraft test was an ambitious attempt to push the state of the art of Doppler Global Velocimetry. The conversion to a system capable of conditionally sampling instantaneous measurements required major changes and additions to the system. Further modifications were also needed for the DGV system to acquire velocity measurements simultaneously with the operation of another optical measurement technology, Projection Moiré Interferometry. Tasks where difficulties were anticipated, such as combining the DGV and PMI systems, synchronizing the lasers, cameras, and data acquisition computers, and conditionally sampling the measurements as a function of rotor azimuth, were achieved successfully. In other areas, however, previous experience was insufficient to predict system performance. These included inadequate frequency control of the Nd:YAG laser, insufficient isolation of the laser and Iodine vapor cells from the tunnel environment, and laser speckle.

While techniques continue to be developed to compensate for the problems with the rotor wake data, improvements in system hardware and data acquisition procedures must be made to avoid these problems. The following improvements comprise the next phase of development:

1) Procedures must be developed to prevent laser damage to wind tunnel models;

2) Active feedback control circuits must be developed to hold the laser optical frequency at a desired point while maintaining stable single frequency laser operation. This improvement applies to both Argon-ion and single-frequency, frequency-doubled Nd:YAG lasers;

3) Optical diagnostic systems must be developed to monitor laser stability. These systems shall provide control signals to the data acquisition system that insure acquisition only when the laser is operating properly;

4) Control software must be developed to automatically calibrate the Iodine vapor cells;

5) The laser must be isolated from harsh wind tunnel environments;

6) Standard Iodine vapor cells must be replaced with vapor limited cells, and better isolated from the wind tunnel environment;

7) Smoke generating systems must be implemented that are capable of completely filling the laser light sheet;

8) Laser light sheet visualization with a continuous-wave laser must be used where necessary to determine proper smoke plume position.

SUMMARY

The on-going development of Doppler Global Velocimetry for application as a wind tunnel flow diagnostic tool has been discussed. The sensitivities of this technology to wind tunnel characteristics and environment have made wind tunnel testing a crucial part of the development process. DGV development is traced from its inception as a laboratory curiosity, to its current three-component configuration capable of conditionally sampling instantaneous measurements. Although many successful innovations have been made, DGV development continues. Remaining problems include laser and Iodine vapor cell stability, automatic determination of stable laser operation, and versatile smoke generating systems.

REFERENCES

1. Komine, H.: *System for Measuring Velocity Field of Fluid Flow Utilizing a Laser -Doppler Spectral Image Converter.* US Patent 4,919,536, 1990.

2. Komine, H.; Brosnan, S. J.; Litton, A. B.; and Stappaerts, E. A.: *Real-time Doppler Global Velocimetry.* AIAA 29th Aerospace Sciences Meeting, Reno, NV, paper AIAA 91-0337, January 7-10, 1991.

3. Meyers, J. F.; and Komine, H.: *Doppler Global Velocimetry - A New Way to Look at Velocity.* **Laser Anemometry: Advances and Applications, 1991**, eds. A. Dybbs & B. Ghorashi, ASME, pp. 289-296, 1991.

4. Meyers, J. F.: *Evolution of Doppler Global Velocimetry Data Processing.* Eighth International Symposium on Applications of Laser Techniques to Fluid Mechanics, paper 11.1, Lisbon, Portugal, July 8-11, 1996.

5. Meyers, J. F.: *Doppler Global Velocimetry – The Next Generation?*. AIAA 17th Aerospace Ground Testing Conference, Nashville, TN, Paper AIAA 92-3897, July 6-8, 1992.

6. Mie, G.: *Optics of Turbid Media*. Ann. Phys. Vol 25, pp. 377-445, 1908.

7. Meyers, J. F.: *Looking at Extremes with Laser Velocimetry*. Proceedings of the 11th International Invitational Symposium on the Unification of Analytical, Computational, and Experimental Solution Methodologies, pp. 491-516, Danvers, MA, August, 18-20, 1993.

8. Meyers, J. F.: *Development of Doppler Global Velocimetry for Wind Tunnel Testing*. AIAA 18th Aerospace Ground Testing Conference, Colorado Springs, CO, paper AIAA 94-2582, June 1994.

9. Komine, H.; Brosnan, S. J.; Long, W. H.; and Stappaerts, E. A.: *Doppler Global Velocimetry Development of a Flight Research Instrumentation System for Application to Non-intrusive Measurements of the Flow Field*. NASA Report CR-191490, 1994.

10. Elliott, G. S.; Mosedale, A.; Gruber, M. R.; Nejad, A. S.; and Carter, C. D.: *The Study of a Transverse Jet in a Supersonic Cross-Flow Using Molecular Filtered Based Diagnostics*. AIAA/ASME/SAE/ASEE 33rd Joint Propulsion Conference and Exhibit, Seattle, WA, paper AIAA 97-2999, July 1997.

11. Roehle, I.: *Doppler Global Velocimetry, Technique and Applications*. Proceedings of the von Karman Institute Lecture Series on Advanced Measurement Techniques, April 6-10, 1998.

12. Meyers, J. F.; Fleming, G. A.; Gorton, S. A.; and Berry, J. D.: *Instantaneous Doppler Global Velocimetry Measurements of a Rotor Wake: Lessons Learned*. 9th International Symposium on Applications of Laser Techniques to Fluid Mechanics, Lisbon, Portugal, paper 1.1, July 13-16, 1998.

13. Fleming, G. A. and Gorton, S. A.: *Measurement of Rotorcraft Blade Deformation using Projection Moiré Interferometry*. Proceedings of the 3rd International Conference on Vibration Measurements by Laser Techniques, Ancona, Italy, June 16-19, 1998.

14. Smith, M. W.: *Application of a Planar Doppler Velocimetry System to a High Reynolds Number Compressible Jet*. AIAA 36th Aerospace Sciences Meeting & Exhibit, paper AIAA 98-0428, Reno, NV, January 12-15, 1998.

15. McKenzie, R. L.: *Planar Doppler Velocimetry for Large-Scale Wind Tunnel Applications*. AGARD Fluid Dynamics Panel 81st Meeting and Symposium on Advanced Aerodynamic Measurement Technology, paper 9, Seattle, WA, September 22-25, 1997.

16. Meyers, J. F.: *Development of Doppler Global Velocimetry as a Flow Diagnostics Tool*. Measurement in Fluids and Combustion Systems, Special Issue, Measurement Science and Technology, vol. 6, no. 6, pp. 769-783, June 1995.

17. Astola, J. and Kuosmanen, P.: **Fundamentals of Nonlinear Digital Filtering**. CRC Press, New York, 1997.

18. Stepniewski, W. Z. and Keys, C. N.: **Rotary-Wing Aerodynamics**. Dover Publications, Inc., New York, 1984.

19. Ghee, T. A.; Berry, J. D.; Zori, L. A. J.; and Elliott, J. W.: *Wake Geometry Measurements and Analytical Calculations on a Small-Scale Rotor Model*. NASA TP-3584, ATCOM TR-96-A-007, August 1996.

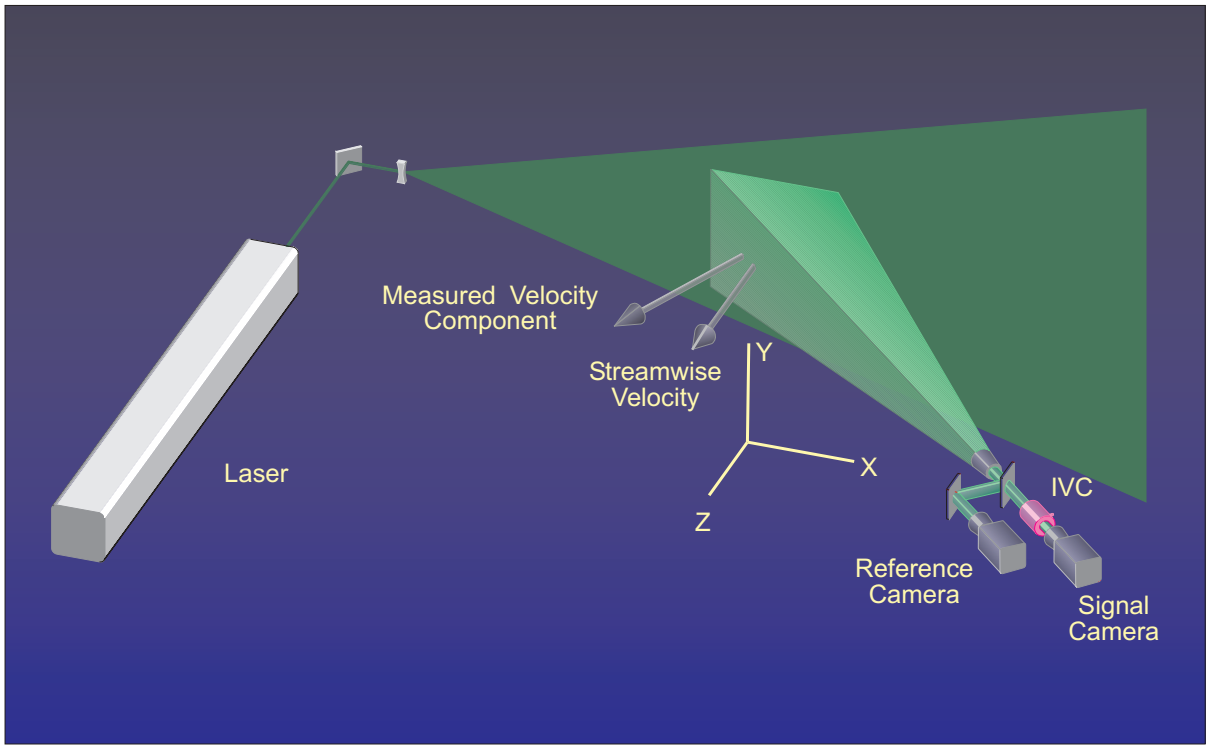

Figure 1.Pictorial view of the Doppler Global Velocimeter used in the Basic Aerodynamics Research Tunnel to measure the flow above a 75° delta wing.

Figure 2. Photograph of the Doppler global velocimeter installed in the Basic Aerodynamics Research Tunnel.

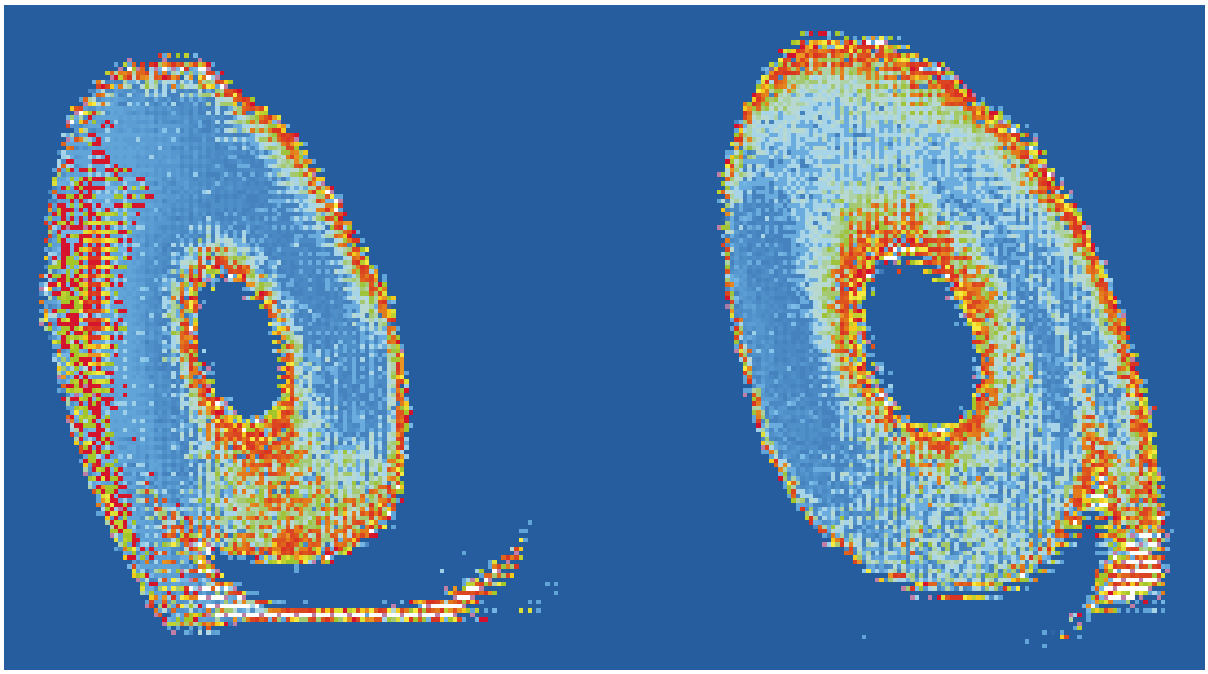

Figure 3. DGV data image for the near cross-flow component of the vortical flow above a 75° delta wing at an angle of attack of 20.5°.

Figure 4. Signal camera image normalized by the reference camera image of the dot target.

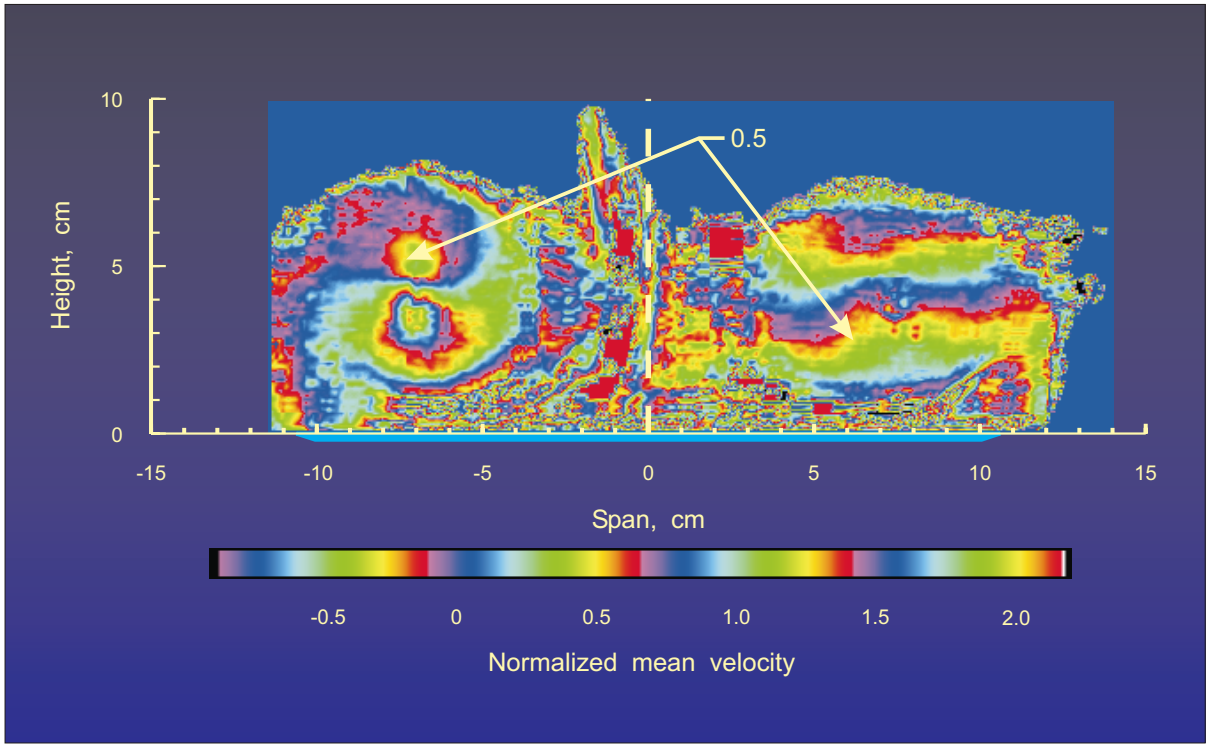

Figure 5. DGV data image for the near cross-flow component of the vortical flow above a 75° delta wing at an angle of attack of 20.5°.

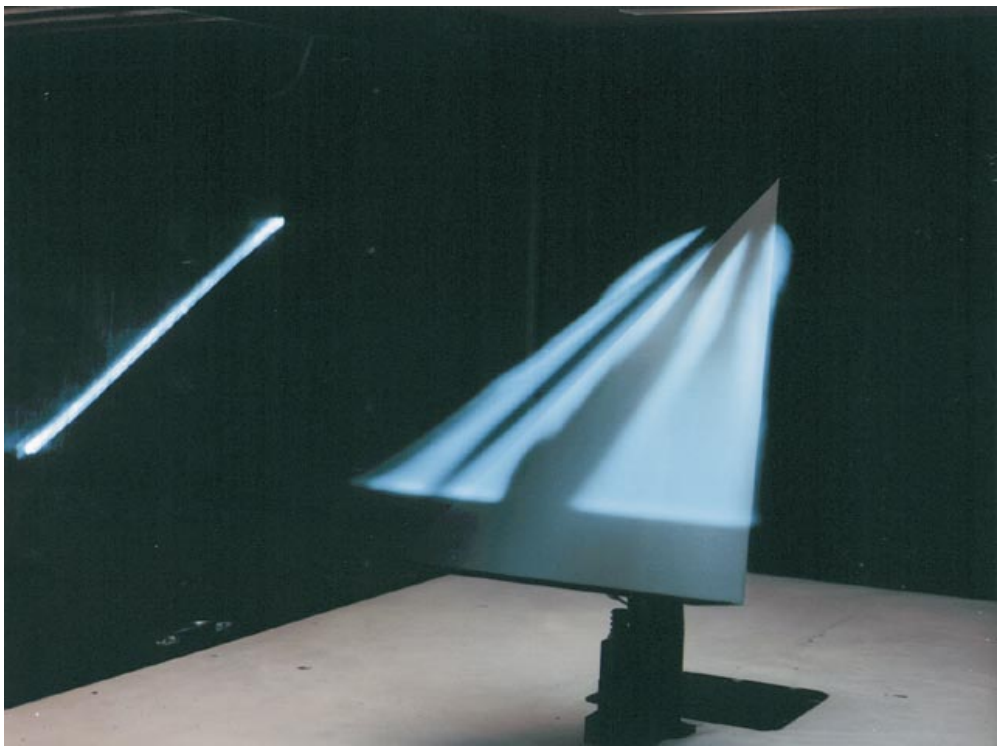

Figure 6. Flow visualization of the vortical flow above a 75° delta wing at an angle of attack of 20.5°.

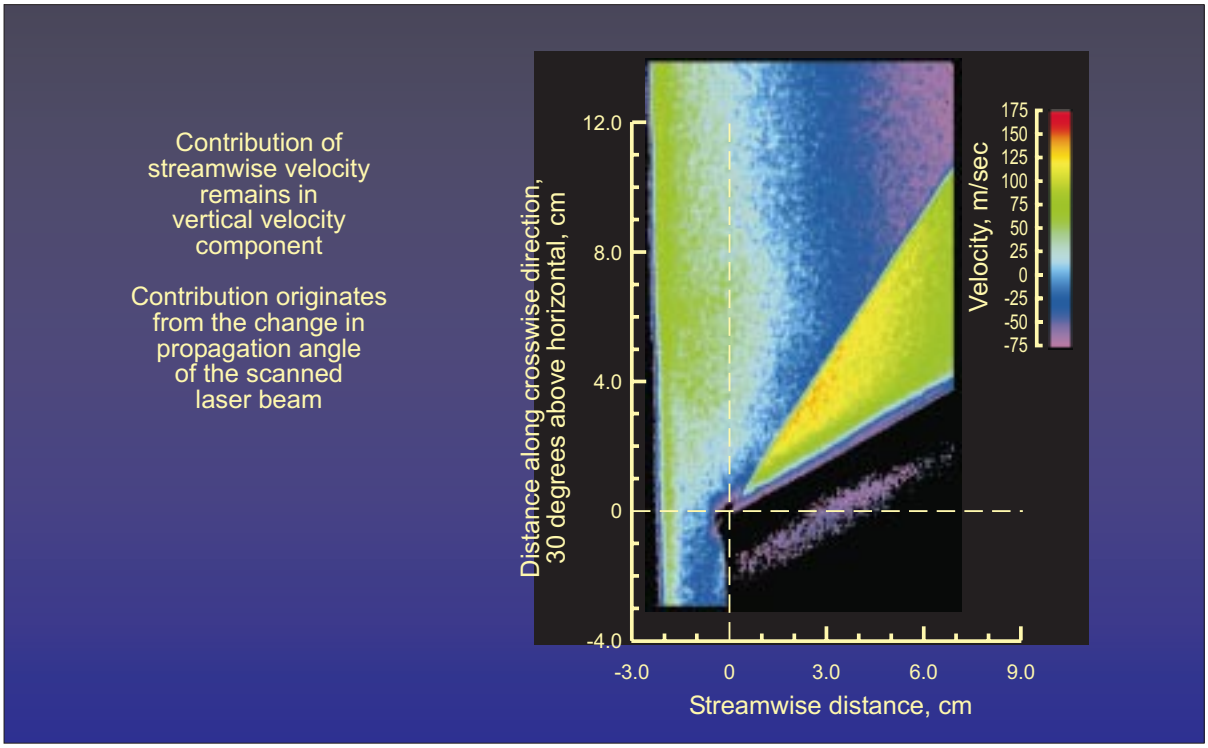

Figure 7. Map of the vertical velocity component measured by the DGV of the flow above a flat plate inclined to -15° at Mach 2.5. Streamwise velocity contribution remains in data.

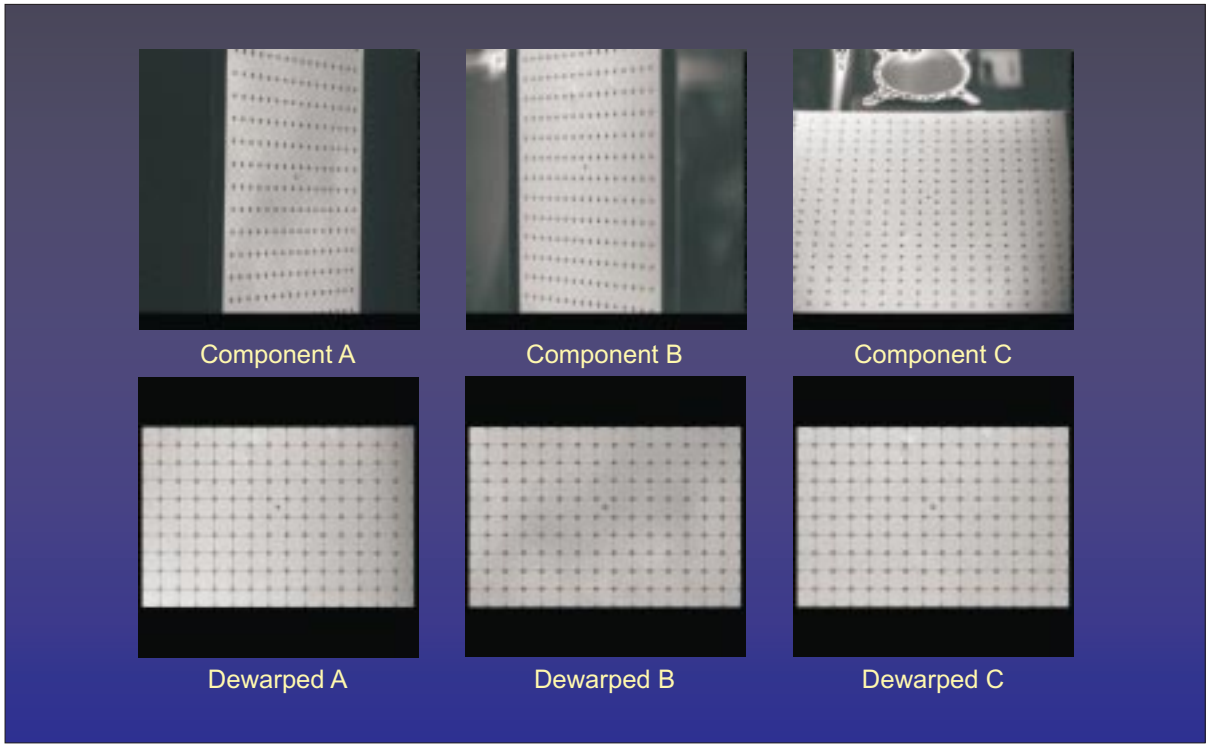

Figure 8. Views of equally spaced dots on a flat card from the left, right, and above with an inclination of 30° from the card plane before and after warping.

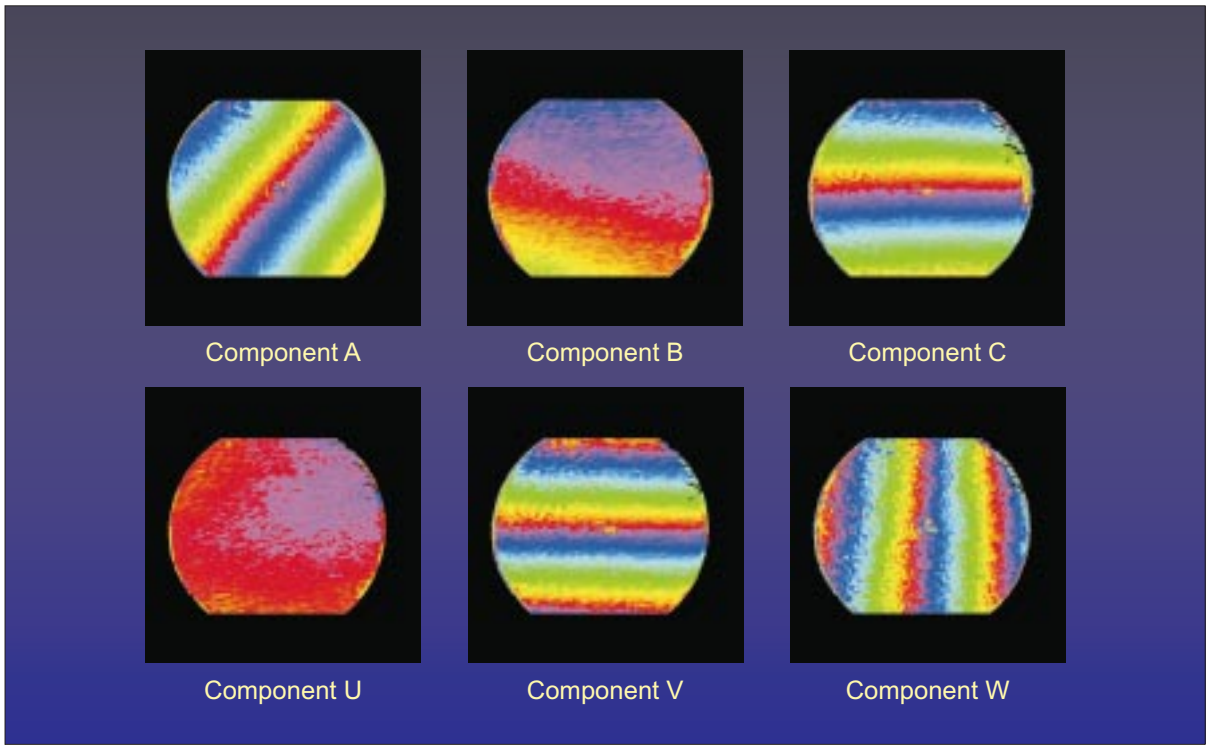

Figure 9. Original and resolved U, V, and W velocity component images of a rotating wheel obtained from the three views shown in figure 8.

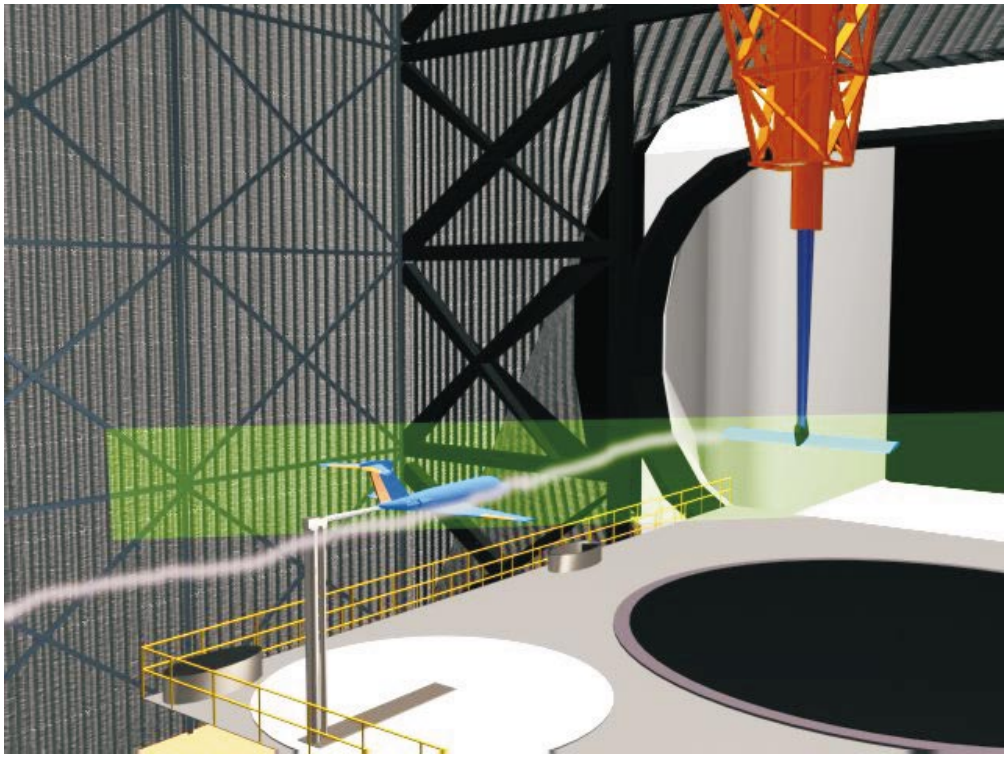

Figure 10.Pictorial view of the wing tip vortex interaction investigation in the Langley 30-x 60-foot Full Scale Wind Tunnel.

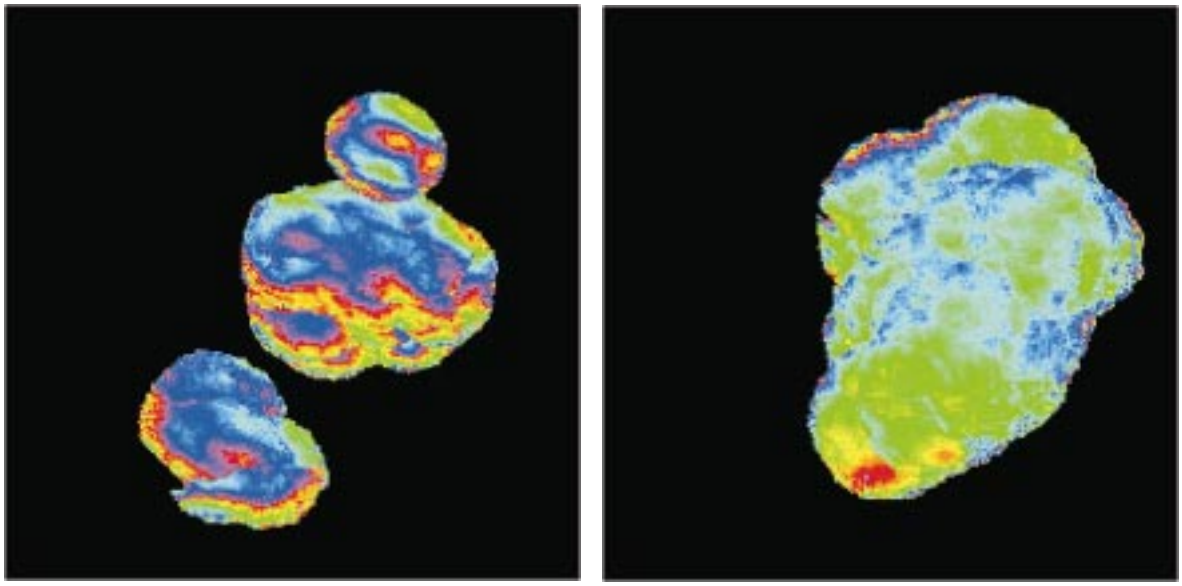

a) angle of attack = 2^{o} b) angle of attack = 10^{o}

Figure 11.Cross flow component velocity mapping of the wing tip vortex, normal average.

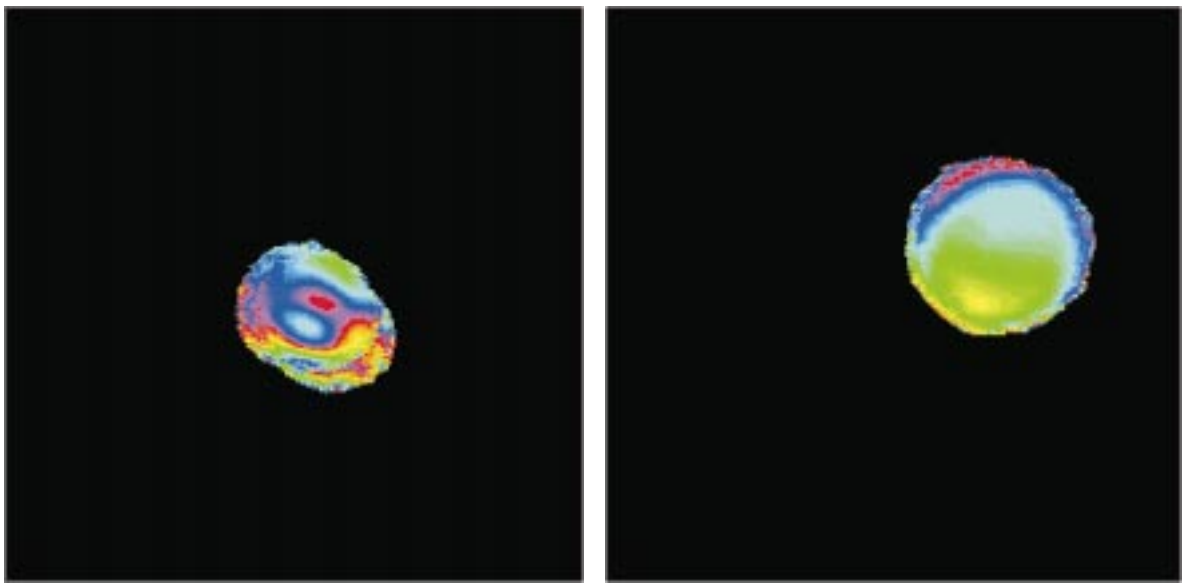

a) angle of attack = 2^{o} b) angle of attack = 10^{o}

Figure 12.Cross flow component velocity mapping of the wing tip vortex, spatially correlated average.

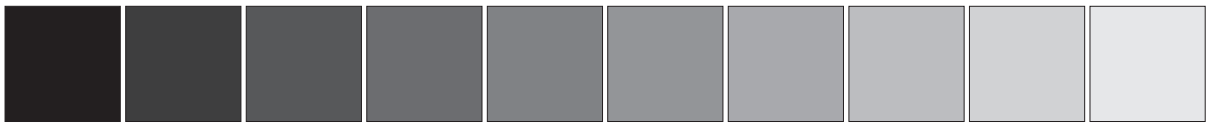

Figure 13.Camera calibration target.

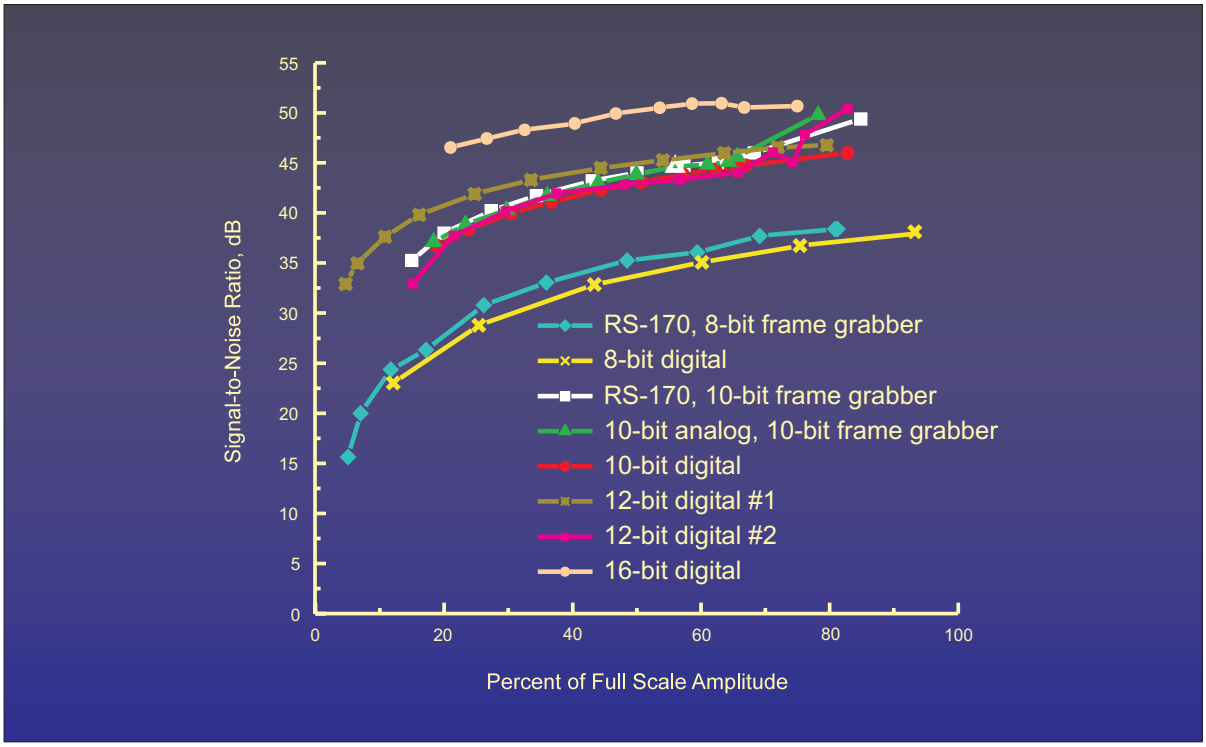

Figure 14. Signal-to-noise ratios for several CCD video camera / frame grabber combinations.

Figure 15. The 1.7-meter isolated rotor system with the fuselage placed below the rotor mounted in the 14-by 22-Foot Subsonic Tunnel.

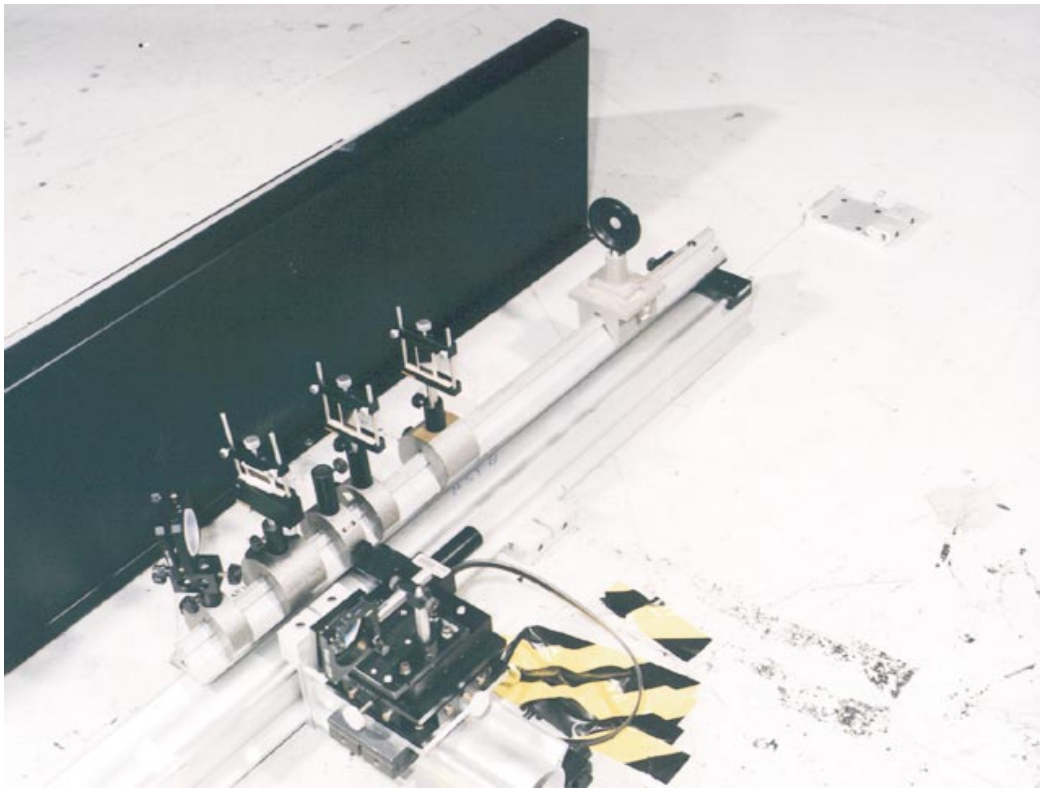

Figure 16. Doppler Global Velocimeter laser light sheet forming optics.

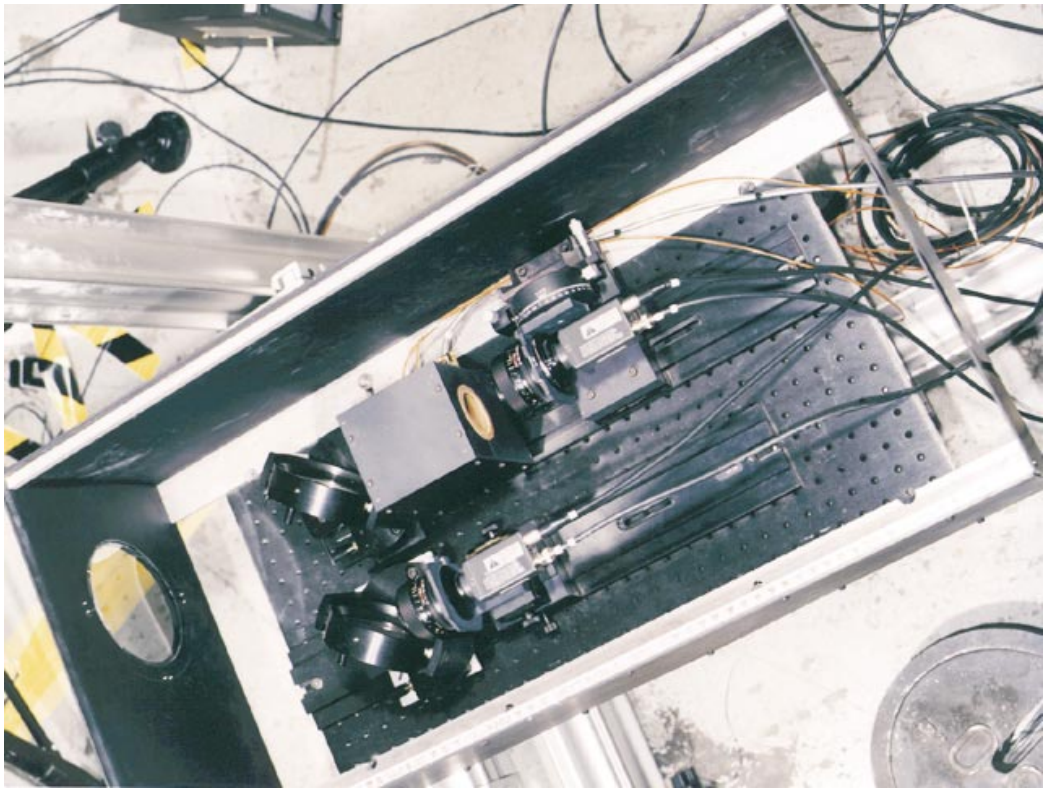

Figure 17. Doppler Global Velocimeter receiver optical system.

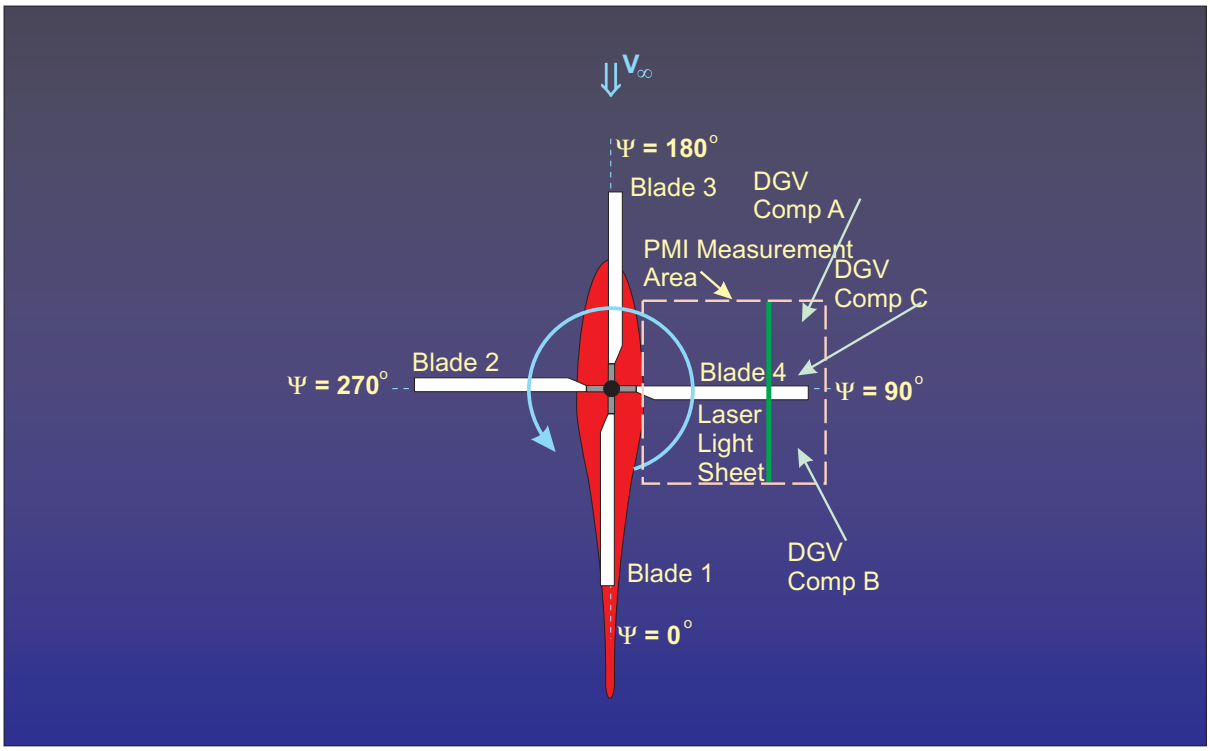

Figure 18. Planview of the model, laser light sheet, DGV receiver optical systems, and PMI measurement area.

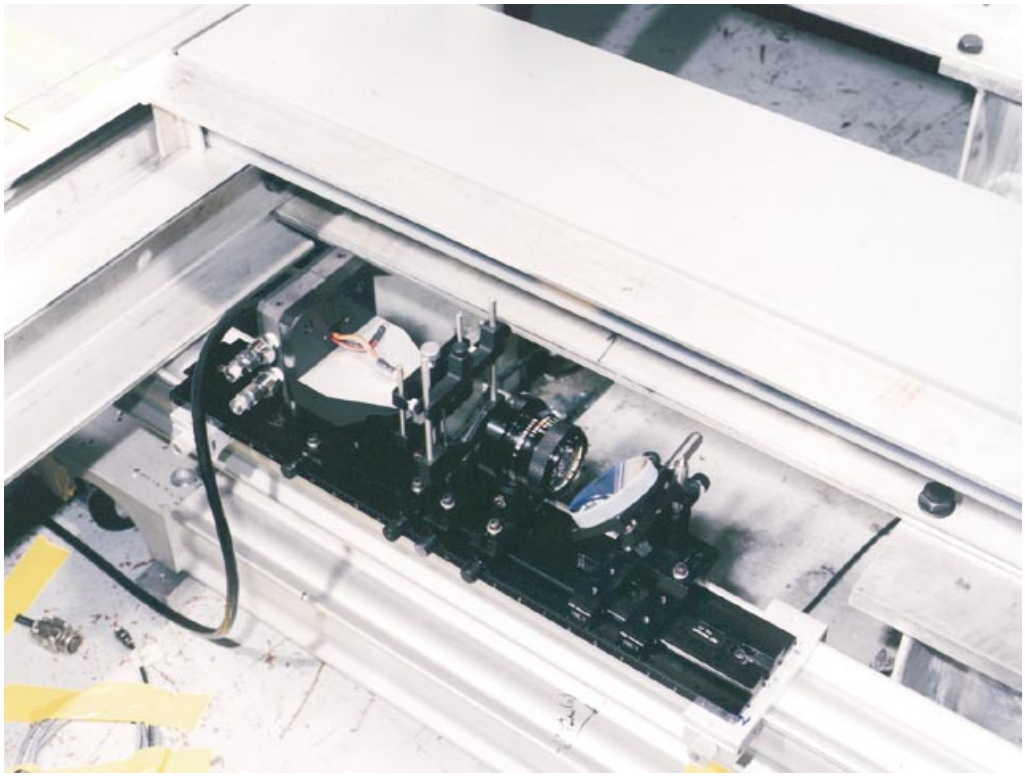

Figure 19. Projection Moiré Interferometer laser and transmission optical system.

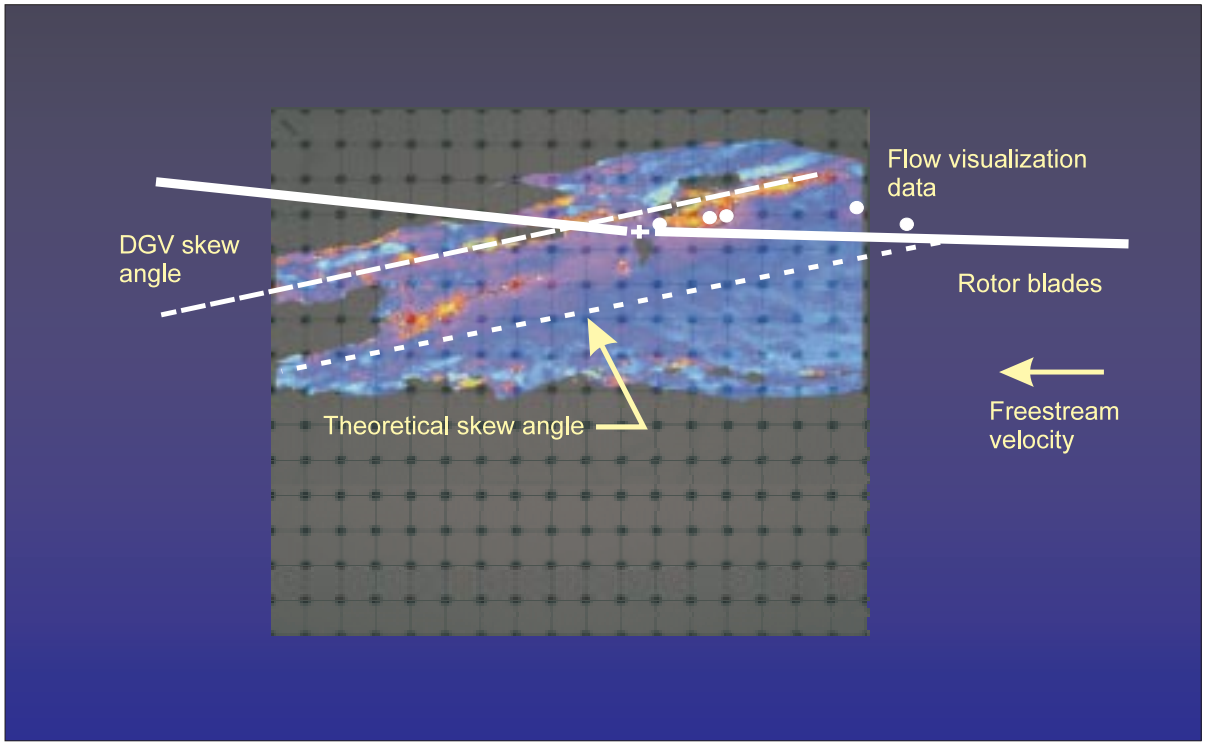

Figure 20. DGV measurement of the streamwise velocity with overlays of theoretical rotor wake skew angle and vortex positions obtained from flow visualization, freestream velocity = 27.7 m/s.

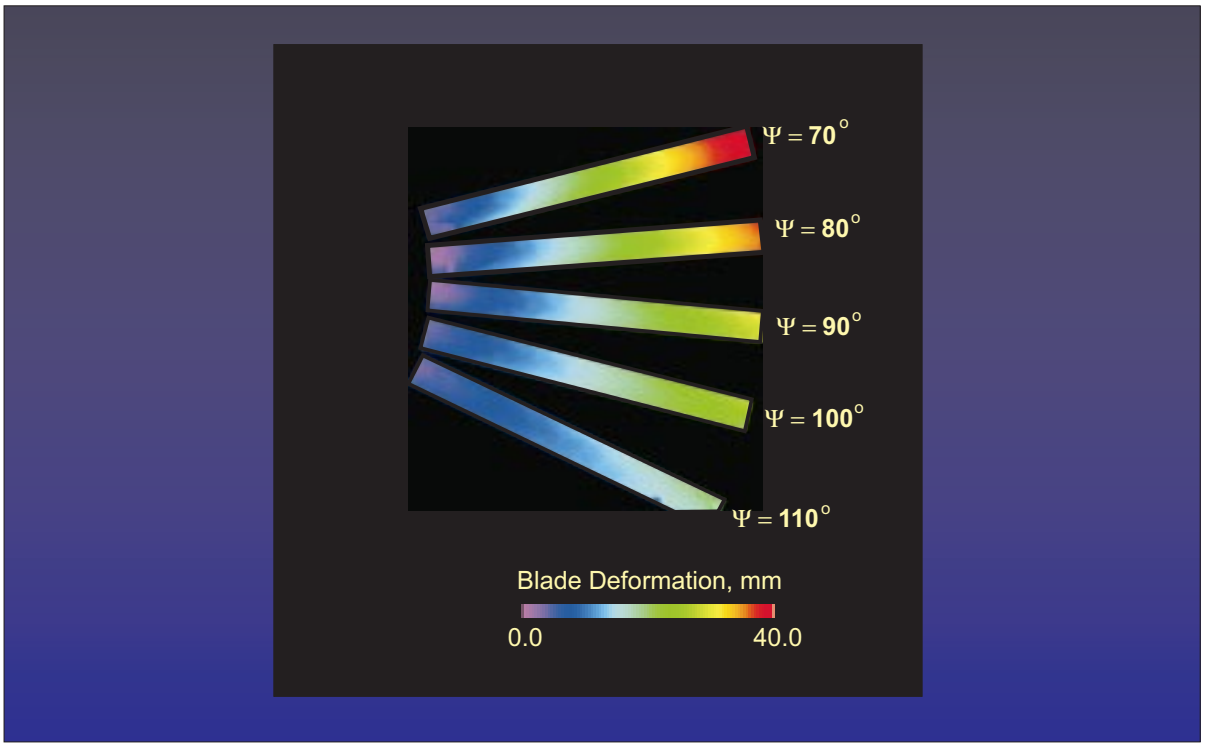

Figure 21. Azimuth dependent PMI measured blade deformation profiles, fuselage down, rotor shaft angle set to -3 degrees.

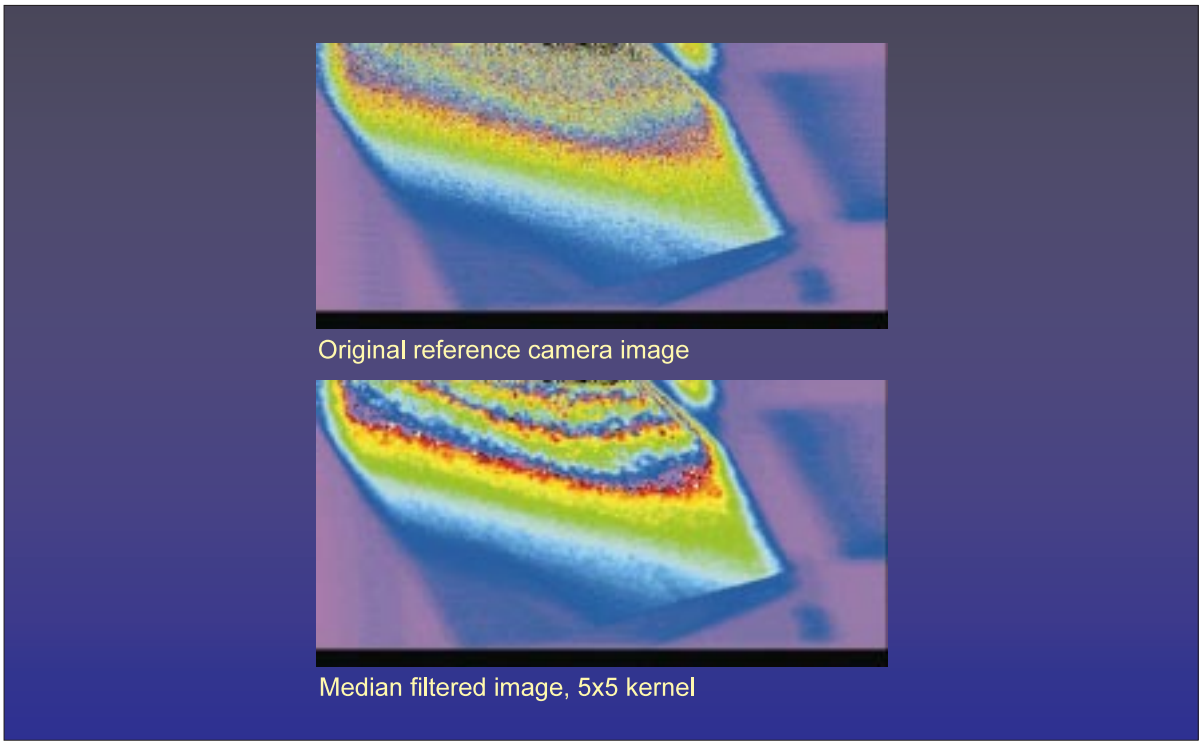

Figure 22.Removal of laser speckle noise with a median filter.

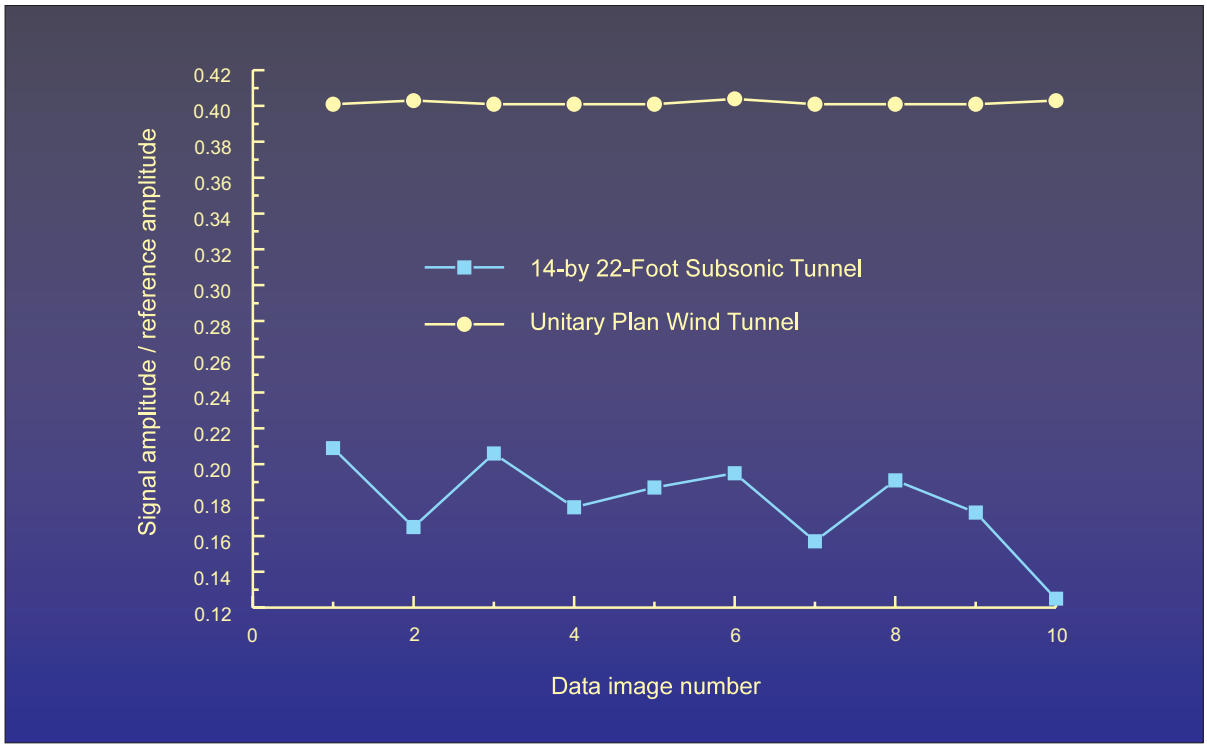

Figure 23.Comparison of Nd:YAG laser frequency stability during two wind tunnel tests.

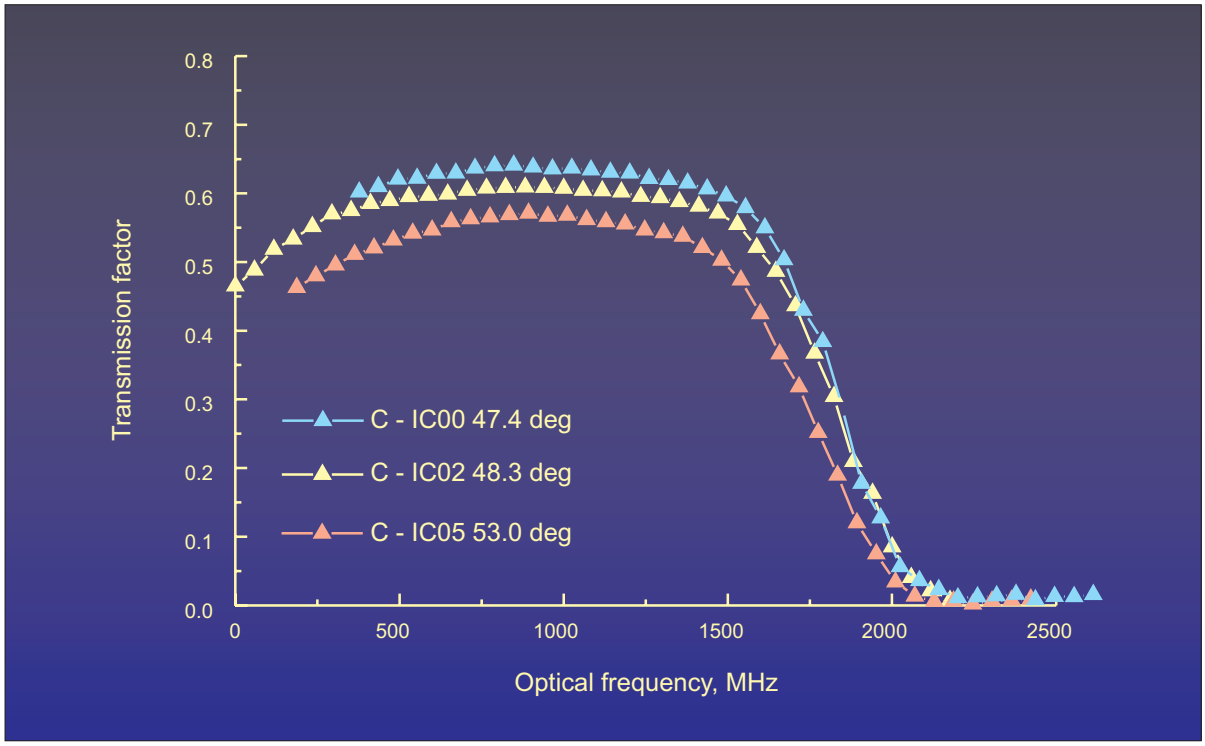

Figure 24.Iodine vapor cell calibratoins for component C before, during, and after a typical run.

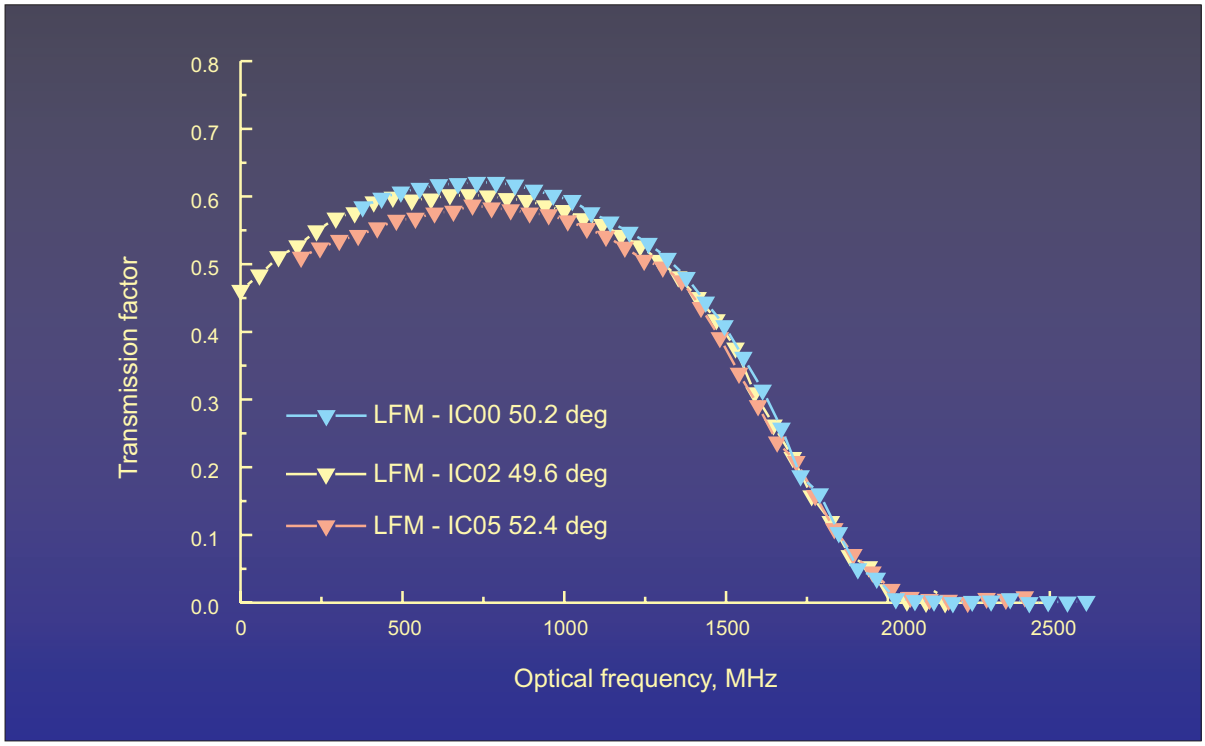

Figure 25.Iodine vapor cell calibrations for the laser frequency monitor obtained simultaneously with Figure 24.